Sea ice in the Baltic Sea during 1993/94–2020/21 ice seasons from satellite observations and model reanalysis

Shakti Singh¹, Ilja Maljutenko¹, and Rivo Uiboupin¹

¹Department of Marine Systems, Tallinn University of Technology, Estonia

Correspondence: Shakti Singh (ssingh@taltech.ee)

Abstract. This study investigates the sea ice characteristics of the Baltic Sea using Copernicus satellite and model reanalysis data products from 1993 onwards. Our primary focus is on assessing the performance of the latest Copernicus model reanalysis product in estimating ice season evolution compared to the satellite dataset. Firstly, the model reanalysis dataset is bias-corrected for further analysis. While the model estimates an earlier start to the ice season, it generally matches satellite data regarding the season's end. Additionally, we find that the model tends to overestimate ice thickness compared to ice chart-based data. Across the Baltic Sea, declining trends for the sea ice are observed. The sea ice characteristics during the recent period (2007/08–2020/21) show decreased sea ice fraction and thickness compared to the preceding period (1993/94–2006/07) of the study. The decrease in the sea ice thickness is over 50 % in some areas during the melting phase. Trend analysis in the study reveals a uniform pattern towards shorter ice seasons (most prominent being in Bothnian Bay with a range of approximately 1–3 days/year of decline in ice season), reduced sea ice extent (SIE) and reduced mean ice thickness (reaching up to -0.4 cm/year).

1 Introduction

The Baltic Sea is a semi–enclosed sea located in Northern Europe, it is recognized as a shelf sea and a marginal sea of the Atlantic. It stands as one of the most extensive brackish water bodies globally (Voipio, 1981). The sea undergoes seasonal fluctuations in ice coverage (Leppäranta and Myrberg, 2009). It stands as a crucial economic zone, hosting one of the world's densest shipping networks and significant economic interests (International Maritime Organization (IMO)). The operations in this region are greatly influenced by the presence of sea ice. Hence, the precise modeling and forecasting of the sea ice season in the Baltic Sea hold significant importance for ensuring secure navigation, particularly for maritime transport, fishing fleets, and various commercial ventures like construction of offshore wind farms. Accurate spatio–temporal observations and predictions also offer important insights into climate patterns, fluctuations in ice coverage, and the broader shifts in the region's environment. During severe winters, Finland and Estonia stand out as the only countries globally where all harbors undergo complete freezing (Jevrejeva and Leppäranta, 2002), an important occurrence that amplifies the priority placed on sea ice studies in the region. The exploration of sea ice dynamics and climatology has been a focal point in numerous studies (Leppäranta, 1981; Haapala and Leppäranta, 1996, 1997; Granskog et al., 2006; Siitam et al. 2017, Raudsepp at al., 2020).

Haapala and Leppäranta in 1996 studied Baltic Sea ice season climatology, using three particular winters (normal, severe. and

mild winters), and concluded that a moderate resolution ice-ocean model could reproduce the main characteristics of the ice season.

The typical duration of the ice season spans up to seven months (Vihma and Haapala, 2009), peaking in late February and early March (BACC II Author Team, 2015), when on average the ice-covered area is 45% of the total area of the Baltic Sea (Leppäranta & Myrberg, 2009). While March usually marks the onset of melting, observations in the northernmost Bothnian Bay have recorded ice persisting until June (Leppäranta and Myrberg, 2009). So the duration of an ice season varies from some 20 to 30 days in the northern Baltic Proper to more than 6 months in the northern Bothnian Bay (Jevrejeva et al., 2004). In the Gulf of Riga sub-basin, the length of ice season observed from remote sensing data is in the range of 3-4.5 months (Siitam et al. 2017). Due to thicker ice and colder climate, ice persists longer in the Bothnian Bay compared to other sub-basins in the Baltic Sea (Pemberton et al., 2017). However, the length of the maximum ice extent period and the temporal dynamics of ice formation or melting, the sub-basins Bothnian Bay, Bothnian Sea, Gulf of Finland, and the Gulf of Riga show a coherent pattern of the interannual variability (Raudsepp et al., 2020). BACC II Author Team, 2015 showed that the sea ice extent and thickness exhibit substantial interannual variability. Time series data analysis on maximum annual SIE and the duration of the ice season suggests a trend towards milder winters. In the 20th century, a decreasing trend of 14 to 44 days has been observed in the length of the ice season (Jevrejeva et al., 2004). A shift in the ice season regime from 2008 was reported which resulted in ice cover and season length decrease (Pärn et al., 2022). In the previous decade (2011–2020), a decrease in the duration of the sea-ice melting was observed and in all sub-basins of the Baltic Sea, a rapid warming during spring was detected (Pärn et al., 2022). Remote sensing techniques have evolved to enhance the efficacy of ice information services (Karvonen 2013; Karvonen 2017; Karvonen 2021; Leppäranta and Lewis, 2007; Mäkynen and Hallikainen, 2005). The studies regarding sea ice in the Baltic Sea have utilized different datasets. In the 2004 study, Jevrejeva et al. used the station data, whereas in a recent study by Pärn et al., 2022, datasets from Copernicus Marine Environment Monitoring Service (Von Schuckmann et al., 2018) and ERA5 (Hersbach, 2020) of European Centre for Medium-range Weather forecast (ECMWF) were used. Nevertheless, remote sensing techniques offer restricted insights into sea ice thickness. Hence model reanalysis data have been utilized for the sea ice thickness analysis.

The Copernicus Marine Service (or Copernicus Marine Environment Monitoring Service) is the marine component of the Copernicus Programme of the European Union. It provides free, regular, and systematic authoritative information on the state of the Blue (physical), White (sea ice), and Green (biogeochemical) ocean, on a global and regional scale. The analysis has utilized the latest model reanalysis Baltic physics product and satellite based products (all described in the upcoming section) from the service for the Baltic Sea. With the recent updates in the regional reanalysis of the Baltic Sea, the new model product has improved spatial resolution and updated sea ice model (Kärna et al., 2021), which provides an improved description of the ice state over previous model products (Panteleit et al. 2019, CMEMS-BAL-QUID-003-011).

50

Objectives: An integral objective of this study was to examine the spatial and temporal disparities between sea ice characteristics from the new release of Copernicus Marine Service Baltic Sea Physics reanalysis product (BALTICSEA_MULTIYEAR _PHY_003_011) to the satellite and ice chart–based datasets. This comparison aims to assess the accuracy of the model

-simulated data in reproducing the observed characteristics of the Baltic Sea ice. The specific objectives are (a) finding the sea ice fraction threshold (TH_SIF) to bias correct (minimize bias) the model reanalysis dataset for sea ice extent (SIE) and comparing ice thickness statistics between the model and SAR & ice charts—based datasets; (b) comparing Baltic Sea Physics reanalysis product's sea ice season evolution characteristics with satellite dataset; (c) analyzing the characteristics and changes of ice extent and thickness during 1993/94–2020/21; (d) providing trend analysis of the sea ice season parameters and sea ice thickness.

2 Datasets

75

The study utilized the Copernicus Marine Sea Surface Temperature (SST) dataset from the reprocessed L4 product which contains Sea Ice Fraction (SIF) data. The Copernicus Marine SST reprocessed L4 product, known as SST_BAL_SST_L4_REP_OBSERVATIONS_010_016 (Høyer et al., 2016) has been developed at the Danish Meteorological Institute (DMI) and offers comprehensive, gap—free maps of sea surface temperature (SST) for the Baltic Sea region. The L4 product is made at a high resolution of 2.4×1.44 km (0.02 °×0.02 °) using satellite data from ESA's SST CCI and Copernicus C3S projects, incorporating an array of different sensors on satellites like NOAA AVHRRs Metop, ATSR1, ATSR2, AATSR, and SLSTR. It also combines this data with in situ measurements from the HadIOD dataset and high—resolution sea ice information from Swedish Meteorological and Hydrological Institute (SMHI) and Finnish Meteorological Institute (FMI). The sea ice fraction data in the product is taken from the sea ice charts from the national ice services at FMI and SMHI, based on manual interpretation by the operator. The product data is available daily from 1 Jan 1982 to 31 Dec 2023. The derived L4 sea surface temperature (SST) used in the product has been compared with different sources of in situ observations by Englyst et al. (2023). Hereafter in the study, this dataset is referred to as the satellite dataset.

The latest reprocessing product (released in March 2023), Copernicus Marine Baltic Sea Physics Reanalysis (BALTIC-SEA_MULTIYEAR_PHY_003_011) have been used in the study. The study utilizes Sea Ice Fraction (SIF) and Sea Ice Thickness (SIT) parameters from this new dataset. The product is based on simulations using the 3D ocean–ice model NEMO (Nucleus for European Modelling of the Ocean) regional Nemo–Nordic 2.0 configuration (Kärna et al, 2021). It offers a comprehensive reanalysis of physical conditions in the Baltic Sea available daily from 1 Jan 1993 to 31 Dec 2021, providing a 2×2 km (0.0277 °×0.0166 °) grid resolution. The physical system assimilates satellite sea surface temperature, in situ temperature and salinity profiles. The system is forced by ECMWF ERA5 meteorology (Hersbach et al. 2020). The fully coupled sea ice model SI3 addresses various aspects of sea ice dynamics, including thermodynamics, advection, rheology, and the processes of ridging and rafting. The land fast ice parametrization utilized in this model follows the approach outlined by Lemieux et al. (2016). The model comprises five ice categories and one snow category, with specified thickness bounds set at 0.45, 1.13, 2.14, and 3.67 m. In this work, the standard settings within the sea ice model, without ice assimilation, originally developed for the global ocean for defining the ice thickness categories, are used. Subsequently in the study, this dataset is referred to as the model dataset.

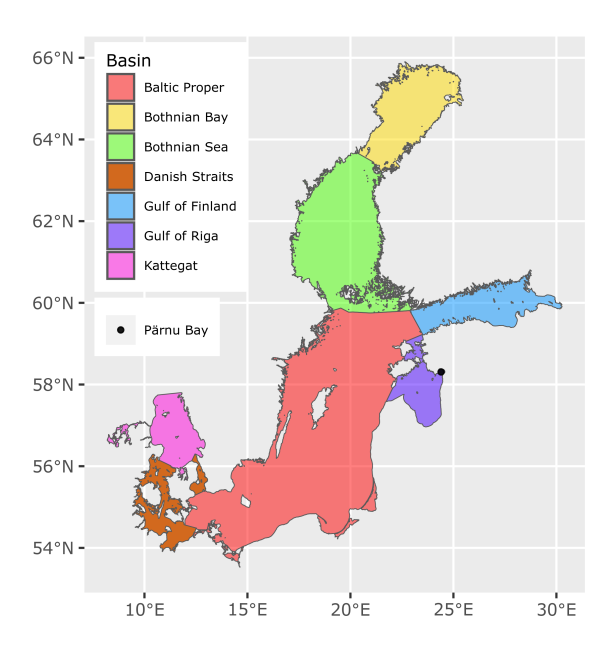


Figure 1. Spatial Distribution of Baltic Sea sub–basins. Figure illustrates the distinct geographical boundaries of Baltic Sea sub–basins–Bothnian Bay (BB), Bothnian Sea (BS), Gulf of Finland (GoF), Gulf of Riga (GoR), Baltic Proper (BP), Danish Straits (DS) and Kattegat–represented in unique colors for differentiation. The sub–basins are based on the PLC–6 project, and are obtained from the Helsinki Commission (HELCOM, 2018)

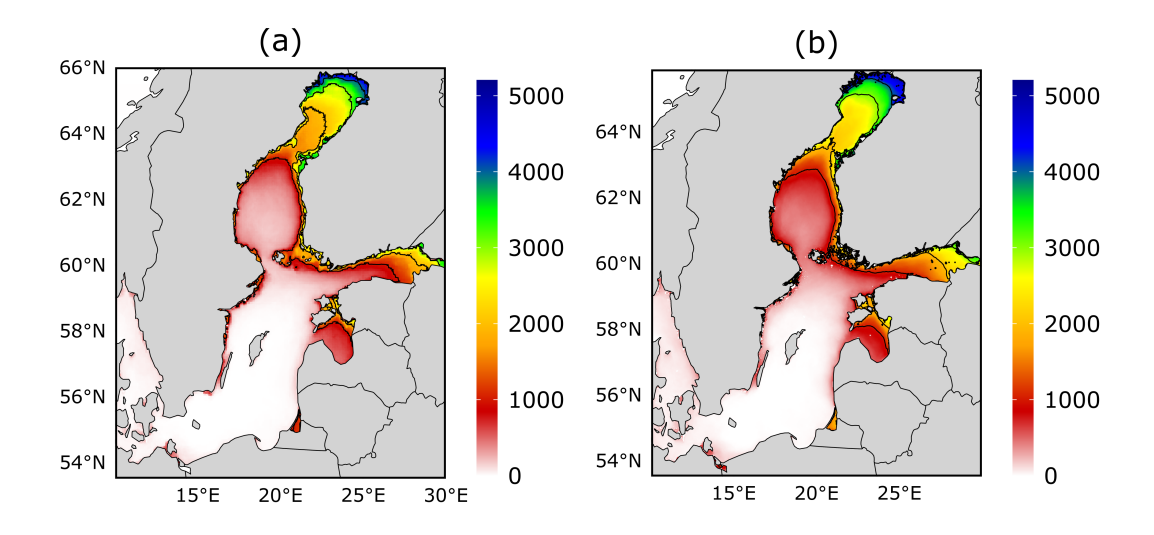


Figure 2. The sample size of the datasets used in the calculations, Panels (a) and (b) illustrate the aggregated days factored into the calculations at individual grid point (solid thin black contour lines are at value of 1000, 2000, 3000, and 4000 days) from satellite and model data respectively

The Copernicus Marine Baltic Sea–Sea Ice Concentration and Thickness Charts product dataset with product id SEAICE _BAL_SEAICE_L4_NRT_OBSERVATIONS_011_004 (Karvonen et al., 2007) has been used in the study to compare the ice thickness statistics with the model dataset. This dataset has 1×1 km spatial resolution and is available daily from 1 Jan 2018 to 5 Jun 2024. The ice parameters in the product are based on SAR image and ice chart produced on a daily basis during the Baltic Sea ice season provided by FMI and SMHI. The product is validated against icebreaker ice thickness data (Berglund et al., 2014) in the Quality Information Document file (CMEMS-SEAICE-QUID-004_011_019, issue 1.1). This is referred to as the SAR & ice charts—based product in the study.

Although ice chart-based sea ice data may have some uncertainties, these datasets have been reliably used in numerous studies to validate other products such as model products (Mäkynen et al., 2020; Karvonen, 2021; Pärn et al., 2021; Leppäranta, 2023) and are available over an extended period. Due to the lack of a better automated tool for interpreting high-resolution sea ice imagery and the limited field observations, ice charts are considered the most accurate datasets for representing the true state of sea ice, and thus other sea ice data sets use them as reference (CMEMS-SI-QUID-011-001to007-009to014, issue 2.10).

The geographical boundaries of the sub-basins used in current study are based on the PLC–6 project, obtained from Helsinki Commision (HELCOM, 2018), shown in Fig. 1. The satellite dataset spans from 1993/94 to 2020/21, the 2012/13 season was excluded (due to the absence of satellite data for the entire season), resulting in a study period covering 27 ice seasons. However, due to the absence of sea ice (absence here refers to sea ice below TH_SIF, explained in the subsequent section) at specific grid points in the Baltic Sea during different years, the data sample size varies across locations. Figure 2 shows this variation, where (a) and (b) represent the sample count of days used in the study. So the calculations of the ice season parameters were based on the data sample size shown in Fig. 2. The procedure employed in the study for calculation of these parameters is given in the subsequent methodology section.

3 Methodology

100

105

110

115

120

The analysis of sea ice statistics in the Baltic Sea region relied on satellite and model datasets, which were used for the calculation of the annual ice season parameters for the study period. For the satellite dataset, a sea ice fraction threshold (TH_SIF) of 0.15 was applied, while the model dataset utilized a TH_SIF of 0.20. The reasoning for choosing these thresholds is given in the subsequent section.

Identification of the onset date of sea ice formation at each grid point (*i*, *j*) was established when the daily mean SIF (*i*, *j*, *d*, *y*) equaled or surpassed the designated TH_SIF from October 1st to March 31st. The **first day** (**FD**) is defined for each year y as the lowest Julian day index (*JDI*) d meeting the TH_SIF criteria within this time range [1]. Conversely, the conclusion date of the sea ice period occurred at grid points where the TH_SIF criteria were last met from January 1st to September 30th. The **last day** (**LD**) is calculated as the highest value of d meeting the criteria within this time range [2]. At each grid, the FD and LD of sea ice are only calculated when there was sea ice observed at those grids (here the occurrence of sea ice for each grid is defined using TH_SIF), hence each grid has a different number of sample sizes (Fig. 2a, 2b) for the calculations of the FD and LD of sea ice. The **total days** (**TD**) of sea ice is the duration between the FD and LD of sea ice occurrence, broadly

representing the **sea ice season** [3]. Conversely, the **number of days** (**ND**) of sea ice specifically accounts for instances within this season that meet the TH_SIF criteria [4].

$$FD(i,j) = \frac{1}{n} \sum_{y=1}^{n} \min(JDI(i,j,y))$$
[1]

Where $JDI = \{d | d \text{ in Range}(October 1st, March 31st), SIF}(i, j, d, y) \ge TH_SIF \text{ in year } y\}$

$$LD(i,j) = \frac{1}{n} \sum_{y=1}^{n} \max(JDI'(i,j,y+1))$$
 [2]

Where $JDI' = \{d \mid d \text{ in Range}(January 1st, September 30th), SIF<math>(i, j, d, y) \ge TH_SIF \text{ in next year } y + 1\}$

$$TD(i,j) = \frac{1}{n} \sum_{y=1}^{n} (\max(JDI'(i,j,y+1)) - \min(JDI(i,j,y)) + 1)$$
[3]

$$ND(i,j) = \frac{1}{n} \sum_{y=1}^{n} count(JDI''(i,j,y))$$
[4]

Where $JDI'' = \{d | d \text{ in Range}(October 1st, September 30th), SIF(i, j, d, y) \ge TH_SIF \text{ in year } y\}$

Comparison between two distinct periods, 1993/1994–2006/2007 and 2007/2008–2020/2021 (hereafter referred to as the preceding period, and recent period respectively), was conducted using 2D histograms. This approach aimed to study the changes in sea ice statistics over the recent 14 year period compared to the preceding 14 year span. Analytical methods included the application of linear regression techniques to discern trends between sea ice parameters within the dataset (the lm function from R, lm is used to fit linear models and can be used to carry out regression). Additionally, the determination of the maximum extent involved computing the integral over the area of the grids where the ice fraction exceeded the designated TH_SIF, serving as an indicator of peak ice coverage during the analyzed periods. A linear trend analysis of the sea ice season parameters and ice thickness has been performed across all the grid points on the Baltic Sea. The products are resampled to a common grid system using bilinear interpolation for comparison. The data sample size is notably higher in the model dataset than in the satellite dataset across the Baltic Sea (Fig. 2). This suggests a more frequent occurrence of sea ice fraction exceeding the threshold (TH SIF) in the model data compared to the satellite data.

145 4 Results

This section is divided into several subsections, including a comparison of the model with satellite sea ice data for ice extent and thickness; an analysis of sea ice season parameters; a statistical examination of sea ice fraction versus sea ice thickness; and a trend analysis of sea ice characteristics.

4.1 Comparison of the model and the satellite dataset

The quality information document (Panteleit et al. 2019, CMEMS-BAL-QUID-003-011) for the Baltic Sea reanalysis product BALTICSEA_MULTIYEAR_PHY_003_011 (https://doi.org/10.48670/moi-00013) validates simulated sea ice statistics against the reference product SEAICE_BAL_SEAICE_L4_NRT_OBSERVATIONS_011_004 (https://doi.org/10.48670/moi-00132) & SMHI ice charts for sea ice concentration and thickness. In the QUID file, the ice extent (mean over all daily values) had a correlation coefficient of 0.94, and the coefficient for ice volume was 0.64. Furthermore, the maximum ice volume estimated from the modeled ice thickness would be around two times greater than the ice volume derived from ice chart data. Concerning our study, a further relevant comparison has been done in the Sect. 4.1.1 & 4.1.2, to minimize the bias for subsequent analysis in the study.

4.1.1 Sea Ice Extent

The sea ice extent (SIE) is calculated by taking an integral over an area of each grid that satisfies the ice fraction threshold criteria. The analysis was aimed at finding out the differences in the SIE between the model reanalysis and the satellite dataset. A threshold value of 0.15 sea ice fraction (SIF) has traditionally been used when computing the sea ice extent (Parkinson, 1987). Hence, in satellite observations, the key TH_SIF was set at 0.15 to calculate SIE. It serves as a crucial point of reference for the study, as the study aimed to determine the appropriate TH_SIF within the model dataset that corresponded accurately to the 0.15 TH_SIF utilized in satellite observations. The comparative analysis of temporal evolution during the ice season for both of these datasets is done for that purpose.

Table 1. Comparison of sea ice extent calculated using different threshold values of SIF for the model dataset is shown by means of statistical methods such as correlation coefficients (CC), root mean square error (RMSE), and mean bias

TH_SIF (Satellite)	TH_SIF (Model)	Bias (km ²)	RMSE (km ²)	CC
0.15	0.10	3476	6574	0.993
0.15	0.15	1783	4887	0.994
0.15	0.20	416	3991	0.995
0.15	0.25	-764	3810	0.996
0.15	0.30	-1820	4193	0.997

The set of SIE estimations was calculated from the model dataset using different SIF_TH and compared to the satellite dataset by means of robust statistics (Table 1). Bias is used as the primary criteria to select optimal threshold, RMSE and CC are calculated to confirm the results. The correlation coefficient values for all the estimations are very high, hence, we focus on the combination that shows the lowest Bias, which happens to be the combination with a sea ice fraction TH_SIF value of 0.20 for the model dataset and 0.15 for satellite observations. This combination of TH_SIF for the datasets shows the minimum bias of 416 km² and the second–lowest RMSE value at 3991 km², in close affinity to the lowest RMSE value (Table 1). The

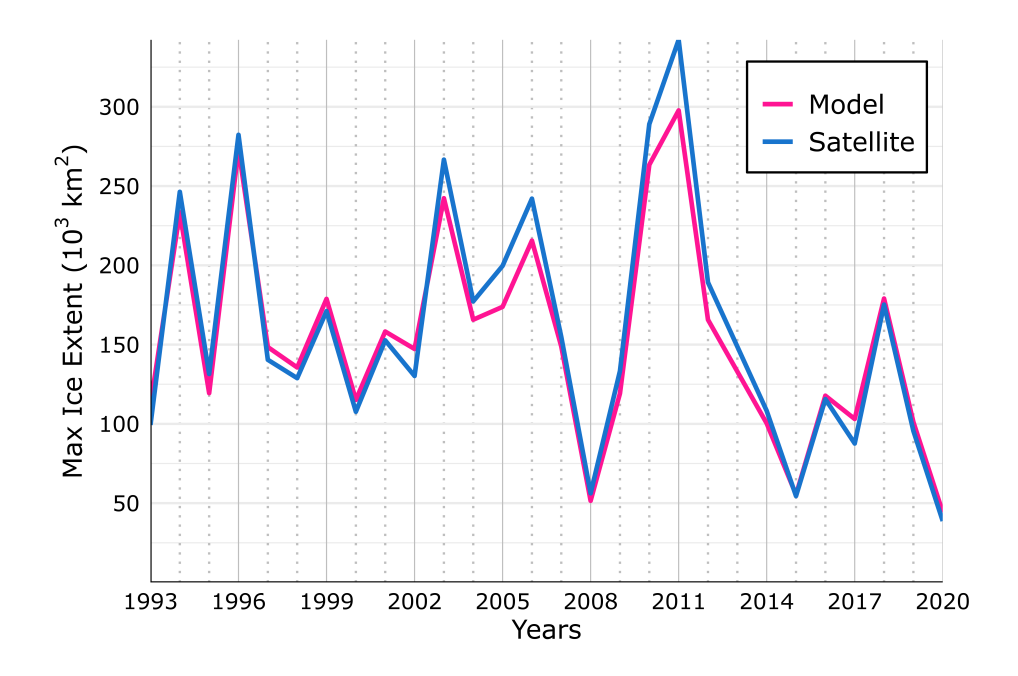


Figure 3. Time series of maximum sea ice cover extent (in 10^3 km^2) in the Baltic Sea across years (1993 to 2020): A comparison between Model (TH_SIF 0.20) and Satellite (TH_SIF 0.15) datasets

selection is based on traditionally used ice fraction thresholds, typically in increments of 0.05, such as 0.15 and 0.20, especially considering 0.20 gives reasonably low bias.

Using TH_SIF of 0.20 may not serve as the optimal approximation for the maximum extent, but we sought to assess its effectiveness in approximating the maximum extent on an interannual scale. This analysis involved plotting the annual maximum ice extent for each year within the study period (Fig. 3). When comparing maximum SIE time series, the bias between the satellite TH_SIF of 0.15 and the model TH_SIF of 0.15 is -1165 km² while the bias between the satellite TH_SIF of 0.15 and the model TH_SIF of 0.20 is -5552 km². Hence TH_SIF of 0.15 for the model dataset, provides more accurate estimates of maximum SIE, while TH_SIF of 0.20 is more suitable for temporal characteristics of the ice season, which is the primary focus of the study, and hence TH_SIF of 0.20 is used for further analysis in the subsequent sections. Despite its shortcomings, this specific combination still exhibits relative consistency in approximating the maximum extent values across the inter–annual scale (Fig. 3). We have used some sea ice season parameters in the subsequent Sect. 4.2 (these parameters have already been defined in the methodology section) to further strengthen our understanding between the two datasets and find out the disparities after using the more suitable TH_SIF for model reanalysis dataset to better depict the satellite observed sea ice season characteristics in the Baltic Sea.

180

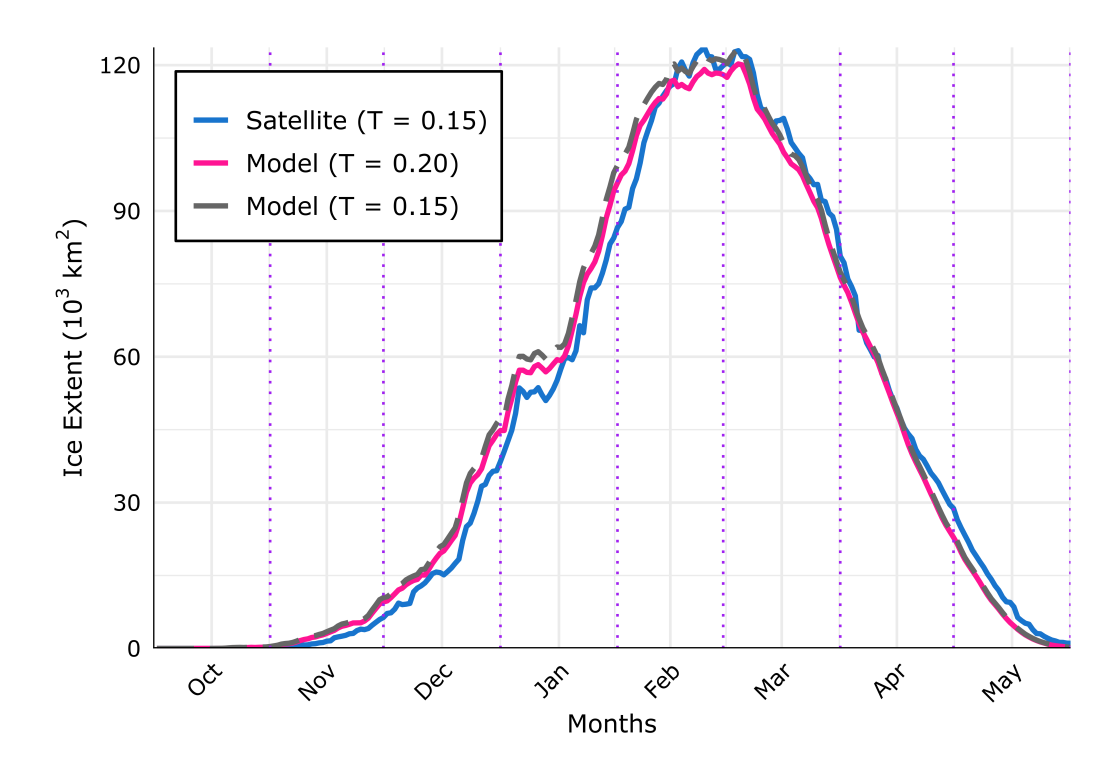


Figure 4. Sea ice season evolution of daily mean sea ice extent (in 10³ km²) in the Baltic Sea (1993/94 to 2020/21): A comparison of Model (TH_SIF 0.20) and Satellite (TH_SIF 0.15) datasets

4.1.2 Sea Ice Thickness

190

The ice thickness data statistics from the model have been compared to SAR image & ice chart based product for three available ice seasons (2018/19, 2019/20 and 2020/21). The model versus observations comparison (Fig. 5) shows that the model overestimates the ice thicknesses by a factor of 1.814, which is consistent with inferences drawn from the QUID file of the model product regarding ice volume. This factor is uniform across different thickness ranges. The model tends to overestimate ice thickness more offshore than near the coasts (Fig. 5 subplot). Despite a high correlation (0.936) the model shows approximately a two–fold overestimation in average thicknesses. The corrected ice thicknesses (by dividing the model ice thickness values by factor 1.814) show a closer resemblance to SAR & ice charts based thicknesses (Fig. 6). After applying the correction factor, the agreement between the model's and SAR & ice charts based ice thicknesses has improved, resulting in minimal differences across the various sub–regions (Fig. 7d).

One of the drawbacks of this analysis is the limitation in data availability, which restricts the comparison of ice thickness to only three winters. It's worth noting that the model reanalysis sea ice thickness data for these three years exhibits considerable variations, with the probability distribution plot (not shown) indicating a similar thickness distribution when compared to the

complete 27-year reanalysis dataset. Additionally, it's important to note that ice charts and SAR-based data tend to saturate at lower thickness values.

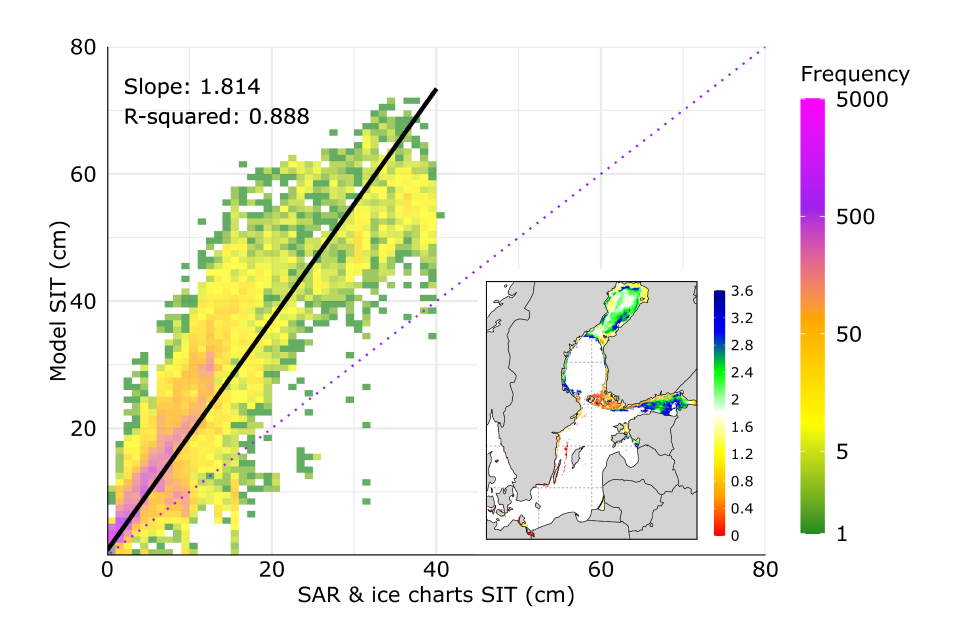


Figure 5. Time averaged sea ice thickness (in cm): SAR & ice charts vs model based dataset. The subplot shows the ratio of time averaged sea ice thickness from model to the SAR & ice charts value

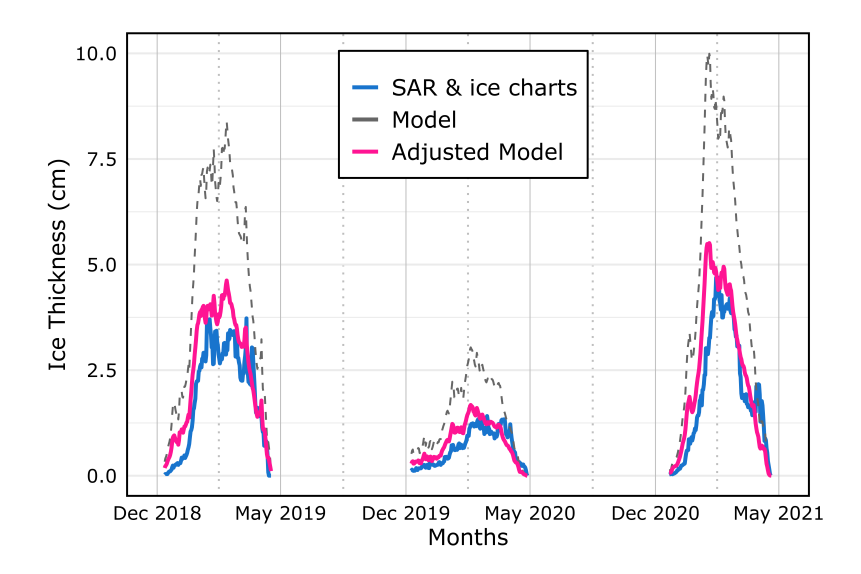


Figure 6. Time series of sea ice thickness spatially averaged over the Baltic Sea for the model and SAR & ice charts based datasets

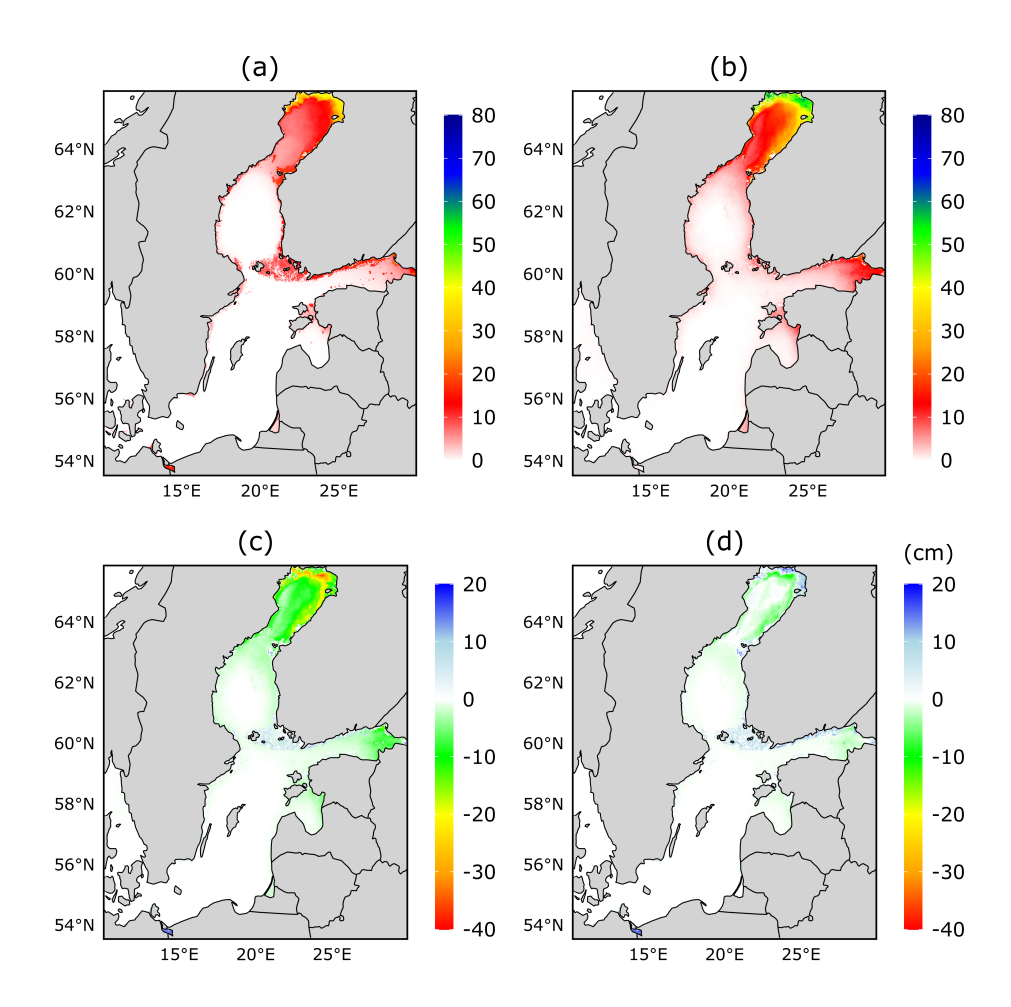


Figure 7. Sea ice thickness, averaged over the three ice seasons (a) from SAR & Ice charts (b) from model (c) model subtracted from SAR & Ice charts (d) adjusted model subtracted from SAR & Ice charts

4.2 Sea Ice Days Characteristics : Satellite vs Model Dataset

205

The spatial distribution of temporal characteristics of the Baltic Sea ice climatology are shown in Figure 8 and a summary of each sub-basin in Table 2. Until the end of December, sea ice is predominantly observed in the northern BB sub-basin (Fig. 8a), and it persists up to May in the northernmost parts (Fig. 8d), resulting in an ice season that lasts approximately 5–6 months in that region (Fig. 8g). Hence, these parts have the largest sample size of the sea ice data for the analysis (Fig. 2a). The sea ice was observed during nearly all the years of the study period for the BB and the eastern GoF sub-basin (Fig. A1). The Bias correction is helpful in correcting or minimizing these errors. For the sea ice, bias correction has been mostly focused on correcting the total sea ice area or extent (Fučkar et al., 2014; Krikken et al., 2016). Bias correcting the models to improve their predictive capabilities of the Baltic Sea ice becomes important for all the winter activities (mentioned in Introduction) in

the region. For example, Pärnu Bay and the region between Estonia and its two major islands, have a longer sea ice season compared to the nearby areas (Fig. 8g). Except for a few years, the sea ice has also been consistently present (more than 80 % of the years) in these parts (Fig. A1).

215

220

225

230

The differences between model and satellite show high spatial variability, specifically in the FD estimates. The model consistently estimates that sea ice starts to form earlier in most parts of the Baltic Sea compared to satellite data (Fig. 8c). This discrepancy is particularly pronounced in the BB, GoF, and GoR sub-basins. On the other hand, the model dataset is more accurate in estimating the end of the sea ice season (Fig. 8f). Modeled LD align better with satellite observations when compared to the FD estimates (Fig. 8f, Table 2). Therefore, earlier FD estimates are causing the overestimation in the modeled TD. The largest discrepancies in TD, similar to the FD between model and satellite, are in the BB and GoF sub-basins (Fig. 8i).

Table 2. Comparative Analysis of Satellite and Model Parameters in Baltic Sea sub-basins. The table compares parameters-FD, LD, TD, and ND-across distinct sub-basins in the Baltic Sea region

Parameters	First Day		Last Day		Total Days		Number of Days	
	Satellite	Model	Satellite	Model	Satellite	Model	Satellite	Model
Bothnian Bay	31 Dec	22 Dec	25 Apr	29 Apr	117	131	103	115
Bothnian Sea	31 Jan	25 Jan	24 Mar	24 Mar	54	61	33	38
Gulf of Finland	19 Jan	9 Jan	1 Apr	31 Mar	73	83	56	65
Gulf of Riga	22 Jan	13 Jan	22 Mar	17 Mar	60	64	41	43
Baltic Proper	12 Feb	10 Feb	1 Mar	2 Mar	20	23	8	9

The ND of the sea ice differs the most from TD in the BS and BP sub-basins (Fig. 8g, 8j), as it depends on the sea ice dynamics within the ice season, such as sea ice drift. The ND disparities between datasets (Fig. 8l) show that the BB and GoF sub-basins exhibit the largest differences. The basin specific ice temporal characteristics (Table 2) are calculated by horizontally averaging sea ice day parameters over the regions shown in Fig. 1. The FD average has a consistent 9–10 day offset towards the early onset date in the model within the BB, GoF, and GoR sub-basins compared to satellite FD. When considering the LD across datasets, a somewhat consistent pattern of ±5 days difference is evident. Consequently, the TD exhibits the most pronounced differences in the BB and GoF sub-basins reaching 14 and 10 days respectively, meanwhile, the BS sub-basin exhibits a noticeable 7 day difference. The ND of sea ice has the largest differences of 12 and 9 days in the BB and GoF sub-basins as well. Therefore, the model consistently overestimates the ice season, mostly due to its tendency to estimate an earlier onset of the ice season.

Contrary to other sub-basins, GoR sub-basin does not display significant discrepancies in ice season length between the two datasets, owing to the model's estimates indicating a forward shift in both the FD and LD of the sea ice season. In line with trends observed in other parameters, the ND of the sea ice value exhibits the highest differences in BB and GoF sub-basins of

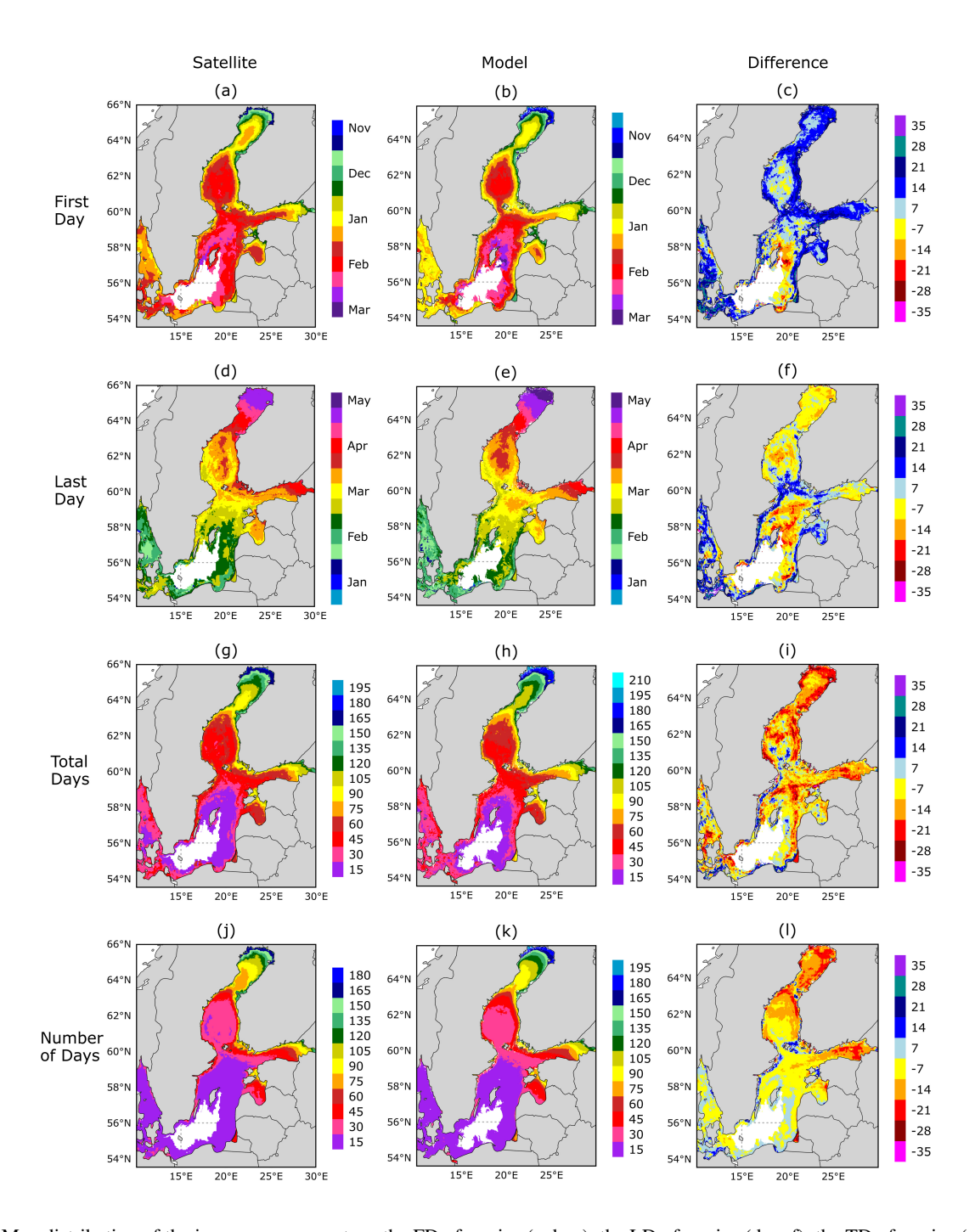


Figure 8. Map distribution of the ice season parameters, the FD of sea ice (a, b, c), the LD of sea ice (d, e, f), the TD of sea ice (g, h, i) and the ND of sea ice (j, k, l). The panels on the left column (a, d, g, j) are from the satellite dataset, the panels in the center column (b, e, h, k) are from the model dataset, and the panels on right column (c, f, i, l) are the differences of the model values from the satellite.

12 and 9 days respectively, while the other sub-basins indicate a closer resemblance between the model dataset and satellite observations for the parameter.

235 4.3 Sea Ice Fraction and Sea Ice Thickness Changes: Model Dataset

240

Based on the regime shift detected by Pärn et al. (2022) we split our study period into two parts: 1993/94–2006/07 (preceding period) and 2007/08–2020/21 (recent period), which allows us to analyze how the sea ice characteristics had changed in these periods. The average max extent has been less in the recent period, and the length of the ice season has also been shorter compared to the preceding period in the Baltic Sea (Fig. 9). The max SIE has decreased from approx. 141×10^3 km² during the preceding period to 109×10^3 km² in the recent period (Fig. 9).

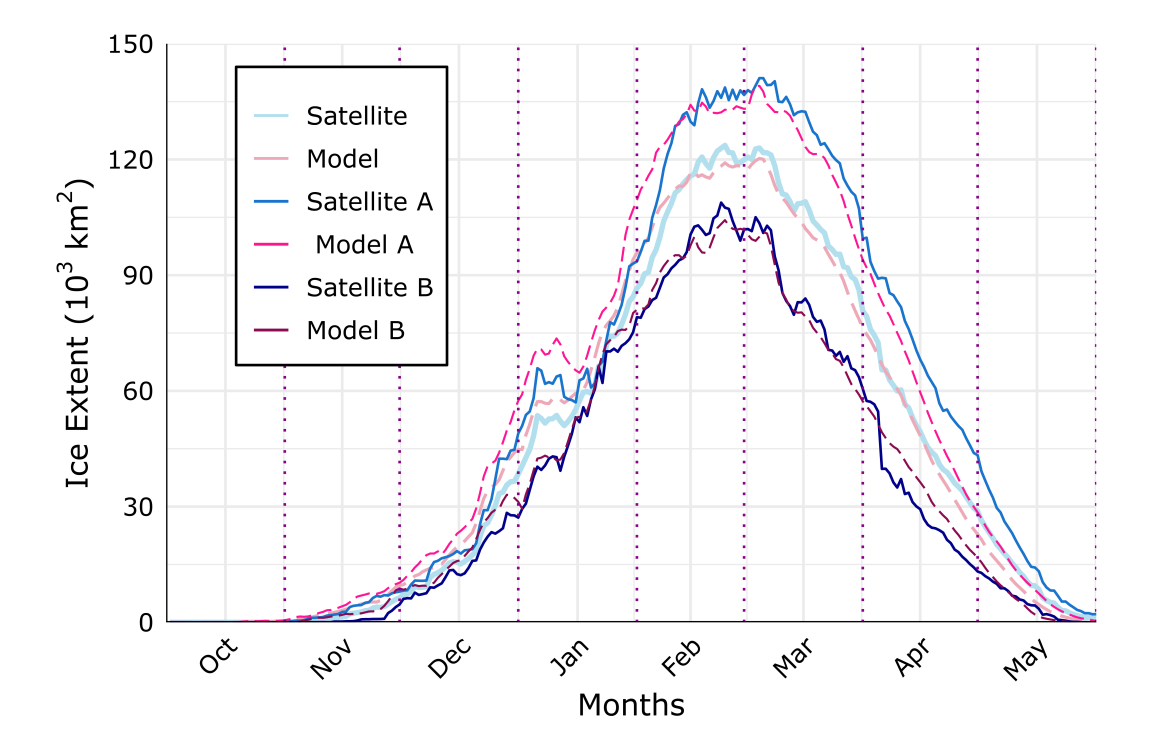


Figure 9. Sea ice season evolution of daily average Baltic Sea ice extent (in 10^3 km²) from 1993/94 to 2020/21: Model (dashed) versus Satellite (solid) datasets, Assessing three periods 1993/94–2006/07, 2007/08–2020/21 (referred as A and B respectively), and the complete 1993/94–2020/21 period

The decrease in SIE is more prominent during the melting period (after the peak SIE), as compared to the ice formation period (before the peak SIE) (Fig. 9). To separately study these changes during sea ice formation and melting, we have divided the ice season into two phases: the freezing phase and the melting phase, as December–January–February (DJF) and March–April–May (MAM) respectively. The date of maximum SIE day varies from year to year, however, its date fluctuates

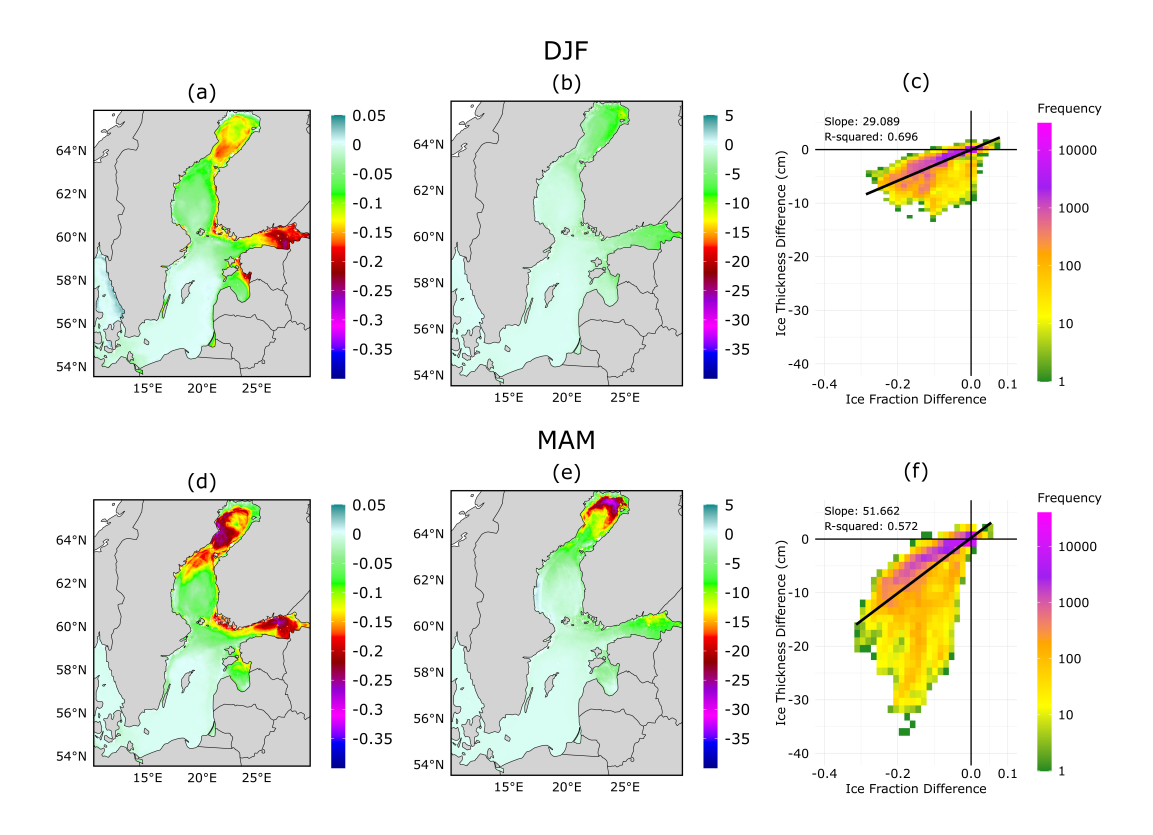


Figure 10. The changes of the SIF and SIT during the recent period 2007/08–2020/21 compared to preceding period 1993/94–2006/07, Panels (a) and (d) show the sea ice fraction (SIF) differences; (b) and (e) the sea ice thickness differences (SIT, in cm); while (c) and (f) shows the 2D histograms plotted for the fraction vs thickness differences, shaded according to their frequency. Linear regression lines are plotted along with their respective slope and r–squared values. Upper panels are for the winter season (DJF), and lower panels are for spring season (MAM)

around the end of February to the beginning of March (Fig. 4). Ice fraction and thickness decreases are higher in the recent period during the melting phase compared to the freezing phase, specifically in the BB sub-basin (Fig. 10d, 10e).

The coherence of the SIF and SIT changes has been shown for the freezing and melting periods in Figs. 10c and 10f. Although the R squared value for both regression lines (which shows how well the data points fit the regression line) is not significant, it still provides us with some surface level information on the sea ice characteristics of the Baltic Sea. The slopes of regression lines suggest that ice thickness has generally decreased more rapidly with a decrease in ice fraction during the melting phase as compared to the freezing phase. From the approximated slopes of regression lines (cm per % of fraction), mean ice thickness decrease during the melting phase is approximately 0.52 cm as opposed to a decrease of 0.29 cm for freezing phase per % change of fraction (Fig. 10c, 10f).

250

255

The sea ice fraction values and their decline in recent period show similar trends for both of the ice season phases (Table 3). Concerning sea ice thickness, the melting phase displays higher ice thickness in the BB sub-basin during the preceding

Table 3. Sub-basin averaged values of Ice Fraction and Ice thickness for both the periods (A & B) during the Freezing phase (DJF) and the Melting phase (MAM). Within the table context, A refers to the preceding period (1993/94–2006/07), while B represents the recent period (2007/08–2020/21)

	DJF				MAM			
Sub-basin	SIF		SIT (cm)		SIF		SIT (cm)	
Period	A	В	A	В	A	В	A	В
Bothnian Bay	0.62	0.50	17.3	12.2	0.67	0.52	34.7	21.5
Bothnian Sea	0.20	0.14	4.1	2.9	0.20	0.11	5.6	3.4
Gulf of Finland	0.44	0.27	10.1	5.4	0.37	0.21	12.1	5.7
Gulf of Riga	0.29	0.20	5.7	3.7	0.20	0.13	5.7	3.3
Baltic Proper	0.03	0.02	0.7	0.5	0.02	0.01	0.5	0.2

Table 4. Changes in sub-basin averaged values of Ice Fraction and Ice thickness in the recent half compared to the preceding during the Freezing phase (DJF) and the Melting phase (MAM)

	DJF				MAM			
Sub-basin	SIF Difference		SIT Difference (cm)		SIF Difference		SIT Difference (cm)	
Bothnian Bay	-0.12	19 %	-5.07	29 %	-0.15	23 %	-13.20	38 %
Bothnian Sea	-0.06	31 %	-1.26	31 %	-0.09	43 %	-2.26	40 %
Gulf of Finland	-0.16	37 %	-4.79	47 %	-0.16	44 %	-6.40	53 %
Gulf of Riga	-0.09	32 %	-2.04	36 %	-0.07	36 %	-2.43	43 %
Baltic Proper	-0.01	29 %	-0.22	31 %	-0.01	47 %	-0.28	56 %

period and notably the most substantial decrease in the sub-basin (Fig. 10e). This occurrence could be attributed to the presence of thicker ice in the BB sub-basin during the melting phase, which could explain the pronounced reduction in ice thickness observed in that area. In percentage terms, even though the melting phase exhibits thicker ice during the preceding period (making it a larger reference value for percentage change), a higher thickness decrease of 38 % during the melting phase compared to a 29 % decrease during the freezing phase in the BB sub-basin is observed. The melting phase has seen a larger decrease of ice fraction and ice thickness compared to the freezing (winter season) phase across all the sub-basins, with the most significant being in the GoF sub-basin, where during the spring season, the ice thickness has reduced to less than half of its value (Table 4). Although our study has not focused on the underlying reasons for these changes, it is evident that recent research has detected rapid warming during the spring season (Pärn et al. 2022). Given that the GoF is a shallow basin, this warming could have contributed to the significant reduction in sea ice observed during the melting phase (spring season). The BP and GoR sub-basins changes reflect the changes in a limited number of winters (Fig. A1) and consequently, particularly in

260

the BP sub-basin, there is a significant reduction in sea ice percentage-wise, but in absolute terms, the decrease is relatively insignificant (Table 4).

4.4 Trend analysis of sea ice characteristics

A linear trend analysis has been performed on each grid cell of the Baltic Sea over the study period for the parameters FD, LD, TD, ND of sea ice and the ice thickness. The resulting spatial distributions of the linear trend across the Baltic Sea are shown in Fig. 11 and Fig. 12.

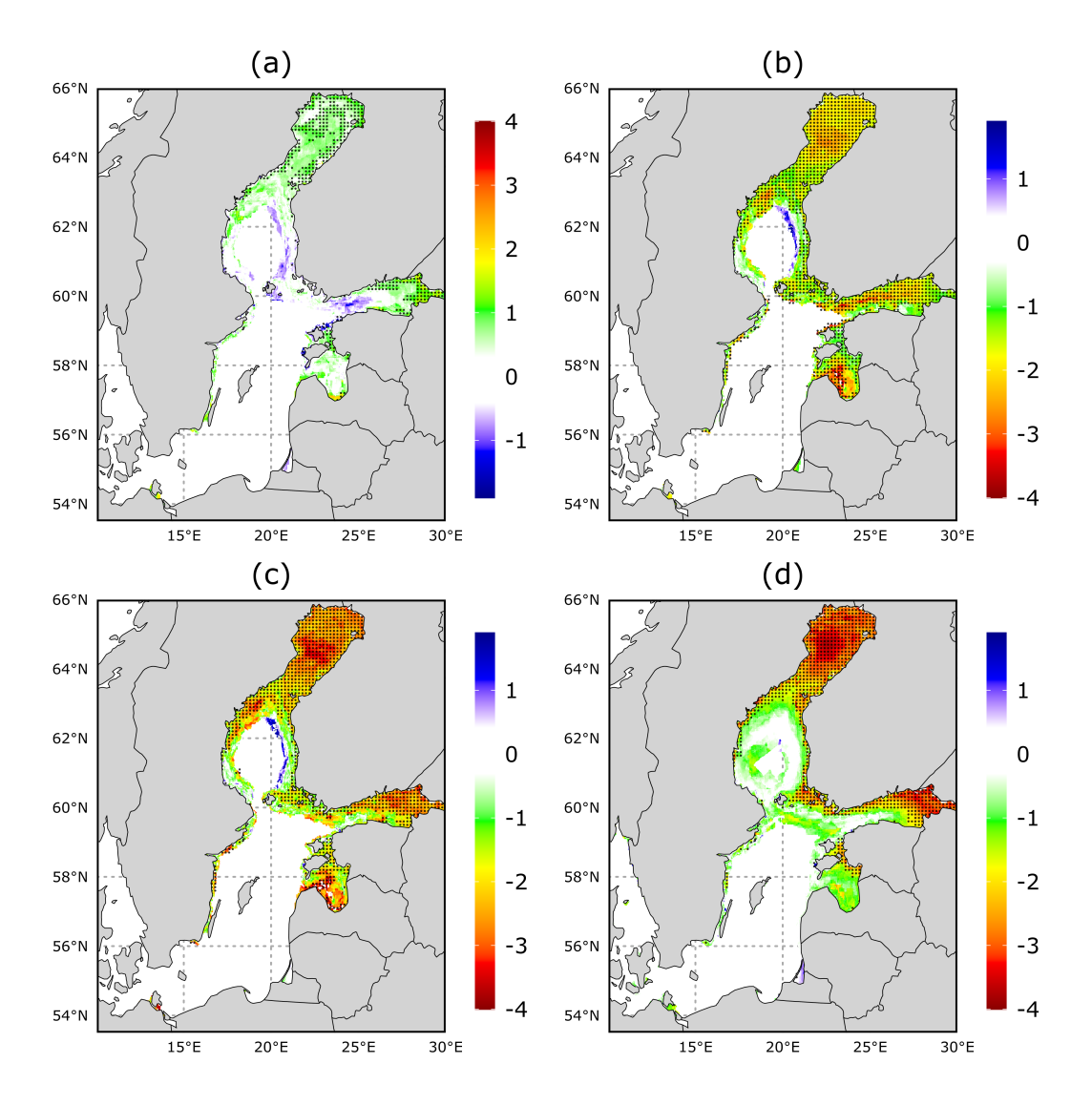


Figure 11. Linear trend for (a) FD (b) LD (c) TD and (d) ND of sea ice (in days/year) during 1993/94 to 2020/21 ice seasons. Black dots mark the areas with 95 % significance level

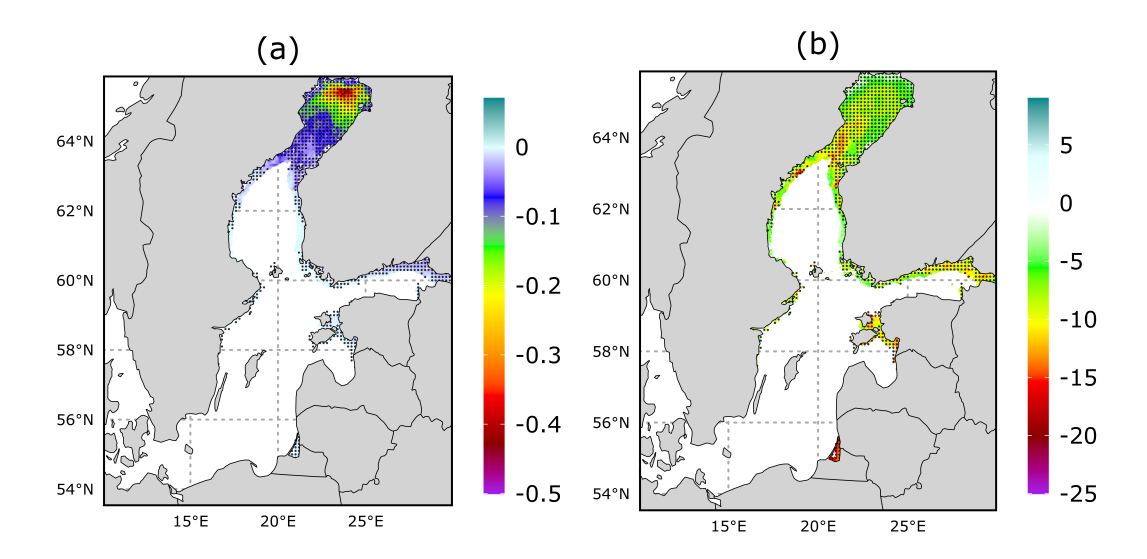


Figure 12. Linear trend for (a) ice thickness (in cm/year) (b) ice thickness (in %) for mean of Nov–May ice thickness from 1993/94 to 2020/21. Black dots mark the areas with 95 % significance level

The FD of sea ice in the Baltic Sea shows an increasing trend, which is statistically insignificant at 95 % significance level for the most parts of the Baltic Sea (Fig. 11a). However, in the case of the LD of sea ice, a decrease of approximately 1–2 days per year above 95 % significance level is observed in almost all parts of BB sub–basin area and in some parts of the GoF sub–basin as well (Fig. 11b). Hence, a decrease of approx. 1–3 days per year in TD and ND of sea ice parameters is observed in roughly the same areas. The linear trends of the annual mean ice thicknesses averaged over ice season (November to May) show that the areas of the northern BB sub–basin have the highest and most significant (over 95 % significance level) decreasing trend of order up to approx. 0.4 cm/year (Fig. 12a). The BB has the highest thickness of sea ice across all the sub–basins (Table 3). The linear trends that are normalized with their respective mean ice thickness show the ice thickness trend in terms of average percentage decrease. The normalized trend values have been uniform over the BB sub–basin standing at approximately -5 percent.

5 Discussion

275

280

The state of sea ice is important for many stakeholders (Wagner et al., 2020). Monitoring the extent and thickness of Baltic ice cover, as well as the duration of the ice season, has been crucial for navigation and travel for centuries. For example, in Finland over 80 % of international trade relies on maritime routes, and ships often require icebreaker assistance for 3 to 6 months each winter (Vihma and Haapala, 2009). Severe sea ice conditions have the potential to substantially disrupt the flow of busy Baltic maritime traffic (Löptien and Axell, 2014). The duration of ice cover in the Baltic Sea significantly impacts spring biota activity, altering the timing of spring blooms and the composition of phytoplankton species (Klais et al., 2017a;

Klais et al., 2017b; Pärn et al., 2021), thereby affecting nutrient cycles and ecosystem dynamics (Klais et al., 2013), which may have significant implications for fisheries industries. To address these needs of various user groups the Digital Twins and their applications for European waters (incl. Baltic Sea) are being developed under the Destination Earth and EDITO (European Digital Twin of the Ocean) initiatives. Thus, accurate information and analysis of sea ice conditions/processes in the Baltic Sea provided in current study over different spatio-temporal scales (from operational monitoring to climate analysis) is also relevant for the development of Digital Twins and related impact models (Åström et al., 2024). The improved sea ice information that can be ingested into the Digital Twins applications and tools enable to carry out what-if scenario analyses and thus improve the planning of offshore activities.

Bias correcting the models to improve their predictive capabilities of the Baltic Sea ice becomes important for all the winter activities (mentioned in previous paragraph) in the region. For the sea ice, bias correction has been mostly focused on correcting the total sea ice area or extent (Fučkar et al., 2014; Krikken et al., 2016). In our study the latest Copernicus Baltic Sea Physics reanalysis product is bias corrected (using a different SIF threshold value) for the mean season evolution of the sea ice extent. For sea ice thickness, satellite product also has uncertainties, and the ice maps only take into account the visible ice thickness from ships when estimating offshore ice thickness. Moreover, they do not contain the additional volume of deformed ice (Raudsepp et al., 2019). Using the SAR imagery & ice charts based Copernicus product for ice thickness could be more suitable, however, it is only available from 2018 onwards. Hence, the model ice thickness was bias corrected using this dataset for the analysis.

300

305

310

320

In the study by Jevrejeva et al. (2004), the long-term time series of date of freezing, breakup, number of days with ice, and maximum annual ice thickness of landfast ice in the Baltic Sea were examined using the station data, and the results provided insights into complicated variability in ice conditions. Their 100 year time series showed a general trend toward reduced ice conditions, with the largest change being the length of the ice season, which has decreased by 14–44 days during the 20th century. Instead of station data (which are mostly onshore), the satellite data provide coverage over the whole Baltic Sea, where we observe a reduced ice season length (on average approx. 1–3 days/year) and decreased maximum SIE (by approx. $32 \times 10^3 \text{ km}^2$) in the recent period (2007/08–2020/21) of our study. As compared to the Jevrejeva et al. (2004) where most of ice season length analysis was done for coastal locations, the current study extends that knowledge to offshore areas as well, for the period 1993/94–2020/2021. The highest reduction in the ice season is also observed at the offshore areas.

The maximum ice extent of the Baltic Sea typically occurs in late February and early March (BACC II Author Team, 2015). It is also supported by our analysis of mean daily extent during ice season, as we observe the mean max SIE in the Baltic Sea during the same time. Due to the larger decrease in SIE after the peak, the changes have been studied for the freezing phase (DJF) and the melting phase (MAM) separately.

A common trend observed is that both the sea ice fraction (correspondingly sea ice extent) and sea ice thickness have decreased in the recent period during both of the ice season phases, specifically, the changes are larger during the spring season, which is in line with the study by Pärn et al. (2022), where they have observed a regime shift during spring time beginning in 2008 in all the basins of the Baltic Sea. For the BB sub-basin, the reduction in sea ice thickness during the melting phase is more pronounced in absolute terms compared to the decrease in sea ice fraction in the study. The possible causes could be

partly attributed to higher sea ice thickness values in the BB during the melting phase in the preceding period of the study. There was no general conclusion concerning maximum annual ice thickness from Jevrejeva et al. (2004), while some sites (Kemi and Kihnu) showed an increase, most time series were characterized by a decreasing trend. During our study period, we observed a significant uniform decreasing trend (about 5 %) in the mean SIT on the northern BB sub–basin, reaching up to 0.4 cm/year in some parts. The value is dependent on the months selected for the annual ice thickness mean. Climatic conditions during the winter months (December–February) largely control the development of the ice cover in the Baltic Sea (Omstedt and Chen, 2001). The reduced ice conditions trends in the Baltic Sea during the 20th century were also related to a warming trend in winter air temperatures over Europe (Jevrejeva et al., 2004). The warming from the present climate leads to a decrease in ice extent by 35–40×10³ km² °C ⁻¹ air temperature change (Leppäranta, 2023). For our study period, these changes could be attributed to global warming and climate change as well. The average air temperature during the study duration has decreased approx. 0.6–0.7 °C (Source: NASA/GISS; https://climate.nasa.gov/vital-signs/global-temperature/), and the average max extent has decreased from approx. 141×10³ km² (33.6 % of the total Baltic Sea) during the preceding period to 109×10³ km² (25.9 %) during the recent period.

The discrepancies in ice models may stem from both atmospheric forcing fields and uncertainties related to the parameterization of ocean–ice–atmosphere processes (Vihma and Haapala, 2009). The majority of state of art models still lack a full atmosphere–wave–ice–ocean coupling system, which inherits various approximations and model corrections through data assimilation. While the correction of the physical model SST using satellite data assimilation helps reduce SST errors in the Nemo–Nordic 2.0 model, the onset of ice periods is still delayed by approximately a week (Fig. 8c). This might mean that there are discrepancies in cooling of sea temperature or errors in early ice formation processes. Given that ice conditions in the Baltic Sea differ from polar regions (e.g. no multi–year ice), bulk parameterizations for ice thermodynamics and rheology processes should be revised according to local ice conditions and ice model should be calibrated using reliable data sources (Pemberton et al., 2017). Additionally, with the development of fine–resolution ice models in dynamic ice regions, it may become relevant to implement more advanced rheology parameterizations, such as brittle ice rheology (Bordeau et al., 2024; Olason et al., 2022).

6 Conclusion

325

330

340

345

355

The study focused on analyzing the Baltic Sea's ice characteristics, utilizing satellite and model datasets. The main findings from the study are given below.

♦ The sea ice statistics (sea ice extent, season length, and mean thickness) from the Copernicus Marine Baltic Sea Physics Reanalysis product (BALTICSEA_MULTIYEAR_PHY_003_011) have been compared with satellite and SAR & Ice charts based statistics. A sea ice fraction threshold of 0.20 for the model dataset provides the most optimal match against the satellite's 0.15 threshold, minimizing bias and root mean square error for the temporal evolution of sea ice extent over the study period. For the ice thickness, compared to SAR & ice charts, the model overestimates its value roughly by a linear factor of 1.814 in the study. During the study period, the model dataset consistently predicts an earlier onset of sea ice but aligns better with satellite

data regarding the end of the ice season. Notable disparities exist in the Bothnian Bay and Gulf of Finland sub-basins,

where the model forecasts longer ice seasons and more sea ice days than the satellite data.

Recent trends showcase decreasing sea ice fraction and thickness in almost every part of the Baltic Sea. Specifically

in the Bothnian Bay, the melting phase exhibits a more rapid decrease in ice thickness per percentage decrease in ice

fraction, compared to the freezing phase. In the Gulf of Finland sub-basin the mean ice thickness has become less than

half of its value during the melting phase in the recent half (2007/08–2020/21) of the study.

♦ The annual mean ice thickness has been decreasing at the highest rate (in absolute terms) in the Bothnian Bay sub–basin

with some northern areas reaching up to approx. 0.4 cm/year, but relative trends of ice thickness thinning have been

nearly uniform (approx. 5 %) across all of the Baltic Sea sub-basins.

Code availability. The codes are available by request via e-mail at shakti.singh@taltech.ee.

Author contributions. SS performed the statistical analysis with input and supervision from IM and RU. RU and IM secured the funding for

the study. SS wrote the first draft, with input from IM and RU. All authors contributed to discussions in writing this paper.

370 Competing interests. The authors declare that they have no conflict of interest.

Acknowledgements. This work was supported by the NOCOS_DT project (NOrdic CryOSphere Digital Twin, VNF23024), funded by

the Nordic Council of Ministers and by AdapEST project (Implementation of national climate change adaptation activities in Estonia,

VEU23019), funded by EU's LIFE programme. The authors are grateful to the Copernicus Marine Service for providing the datasets.

Appendix A: Appendix

360

365

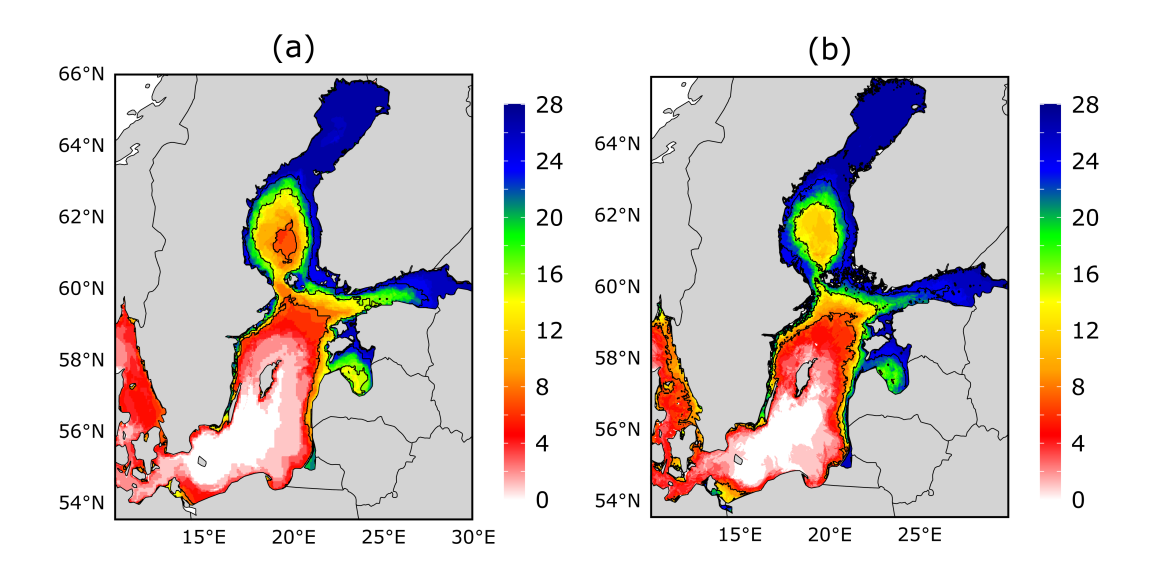


Figure A1. The sample size of the datasets used in the calculations, Panels (a) and (b) illustrate the count of years factored into the calculations (solid thin black contour lines are at value of 8, 16, and 24 years) from satellite and model data respectively

References

375

380

390

Åström, J., Robertsen, F., Haapala, J., Polojärvi, A., Uiboupin, R., and Maljutenko, I.: A large-scale high-resolution numerical model for sea-ice fragmentation dynamics, The Cryosphere, 18, 2429–2442, 2024.

Berglund, R. and Molinier, M.: IceTrafPrep: A feasibility study of a Trafficability Ice Chart Service, 2014.

Brodeau, L., Rampal, P., Ólason, E., and Dansereau, V.: Implementation of a brittle sea ice rheology in an Eulerian, finite-difference, C-grid modeling framework: impact on the simulated deformation of sea ice in the Arctic, Geoscientific Model Development, 17, 6051–6082, 2024.

Collins, M.: Climate predictability on interannual to decadal time scales: The initial value problem, Climate dynamics, 19, 671–692, 2002. Director, H. M., Raftery, A. E., and Bitz, C. M.: Improved sea ice forecasting through spatiotemporal bias correction, Journal of Climate, 30, 9493–9510, 2017.

E.U. Copernicus Marine Service Information (CMEMS): Baltic Sea Physics Reanalysis, Marine Data Store (MDS), dOI: 10.48670/moi-00013, Accessed on 01 Dec 2023a.

E.U. Copernicus Marine Service Information (CMEMS): Baltic Sea - Sea Ice Concentration and Thickness Charts, Marine Data Store (MDS), dOI: 10.48670/moi-00132, Accessed on 01 Dec 2023b.

E.U. Copernicus Marine Service Information (CMEMS): Baltic Sea- Sea Surface Temperature Reprocessed, Marine Data Store (MDS), dOI: 10.48670/moi-00156, Accessed on 01 Dec 2023c.

Fučkar, N. S., Volpi, D., Guemas, V., and Doblas-Reyes, F. J.: A posteriori adjustment of near-term climate predictions: Accounting for the drift dependence on the initial conditions, Geophysical Research Letters, 41, 5200–5207, 2014.

Granskog, M., Kaartokallio, H., and Shirasawa, K.: Nutrient status of Baltic Sea ice: Evidence for control by snow-ice formation, ice permeability, and ice algae, Journal of Geophysical Research: Oceans, 108, 2003a.

- 395 Granskog, M., Kaartokallio, H., Kuosa, H., Thomas, D. N., and Vainio, J.: Sea ice in the Baltic Sea-a review, Estuarine, Coastal and Shelf Science, 70, 145–160, 2006a.
 - Granskog, M. A., Martma, T. A., and Vaikmäe, R. A.: Development, structure and composition of land-fast sea ice in the northern Baltic Sea, Journal of Glaciology, 49, 139–148, 2003b.
- Granskog, M. A., Vihma, T., Pirazzini, R., and Cheng, B.: Superimposed ice formation and surface energy fluxes on sea ice during the spring melt–freeze period in the Baltic Sea, Journal of Glaciology, 52, 119–127, 2006b.
 - Haapala, J. and Leppäranta, M.: Simulating the Baltic Sea ice season with a coupled ice-ocean model, Tellus A, 48, 622-643, 1996.
 - HAAPALA, J. and LEPPÄRANTA, M.: The Baltic Sea ice season in changing climate, Boreal environment research, 2, 93–108, 1997.
 - Haapala, J. J., Ronkainen, I., Schmelzer, N., and Sztobryn, M.: Recent change—Sea ice, Second assessment of climate change for the Baltic Sea basin, pp. 145–153, 2015.
- 405 Hazeleger, W., Guemas, V., Wouters, B., Corti, S., Andreu-Burillo, I., Doblas-Reyes, F. J., Wyser, K., and Caian, M.: Multiyear climate predictions using two initialization strategies, Geophysical Research Letters, 40, 1794–1798, 2013.
 - Hersbach, H., Bell, B., Berrisford, P., Hirahara, S., Horányi, A., Muñoz-Sabater, J., Nicolas, J., Peubey, C., Radu, R., Schepers, D., et al.: The ERA5 global reanalysis, Quarterly Journal of the Royal Meteorological Society, 146, 1999–2049, 2020.
 - Høyer, J. L. and Karagali, I.: Sea surface temperature climate data record for the North Sea and Baltic Sea, Journal of Climate, 29, 2529–2541, 2016

- Høyer, J. L. and She, J.: Optimal interpolation of sea surface temperature for the North Sea and Baltic Sea, Journal of Marine Systems, 65, 176–189, 2007.
- Jakacki, J. and Meler, S.: An evaluation and implementation of the regional coupled ice-ocean model of the Baltic Sea, Ocean Dynamics, 69, 1–19, 2019.
- Jevrejeva, S.: Severity of winter seasons in the northern Baltic Sea between 1529 and 1990: reconstruction and analysis, Climate Research, 17, 55–62, 2001.
 - Jevrejeva, S. and Leppäranta, M.: Ice conditions along the Estonian coast in a statistical view, Hydrology Research, 33, 241–262, 2002.
 - Jevrejeva, S. and Moore, J. C.: Singular spectrum analysis of Baltic Sea ice conditions and large-scale atmospheric patterns since 1708, Geophysical Research Letters, 28, 4503–4506, 2001.
- 420 Jevrejeva, S., Moore, J., and Grinsted, A.: Influence of the Arctic Oscillation and El Niño-Southern Oscillation (ENSO) on ice conditions in the Baltic Sea: The wavelet approach, Journal of Geophysical Research: Atmospheres, 108, 2003.
 - Jevrejeva, S., Drabkin, V., Kostjukov, J., Lebedev, A., Leppäranta, M., Mironov, Y. U., Schmelzer, N., and Sztobryn, M.: Baltic Sea ice seasons in the twentieth century, Climate research, 25, 217–227, 2004.
- Jylhä, K., Fronzek, S., Tuomenvirta, H., Carter, T. R., and Ruosteenoja, K.: Changes in frost, snow and Baltic sea ice by the end of the twenty-first century based on climate model projections for Europe, Climatic Change, 86, 441–462, 2008.
 - Kärnä, T., Ljungemyr, P., Falahat, S., Ringgaard, I., Axell, L., Korabel, V., Murawski, J., Maljutenko, I., Lindenthal, A., Jandt-Scheelke, S., et al.: Nemo-Nordic 2.0: Operational marine forecast model for the Baltic Sea, Geoscientific Model Development, 14, 5731–5749, 2021.
 - Karvonen, J.: Baltic sea ice concentration estimation based on C-band dual-polarized SAR data, IEEE Transactions on Geoscience and Remote Sensing, 52, 5558–5566, 2013.
- 430 Karvonen, J.: Baltic sea ice concentration estimation using SENTINEL-1 SAR and AMSR2 microwave radiometer data, IEEE Transactions on Geoscience and Remote Sensing, 55, 2871–2883, 2017.

- Karvonen, J.: Baltic sea ice concentration estimation from c-band dual-polarized sar imagery by image segmentation and convolutional neural networks, IEEE Transactions on Geoscience and Remote Sensing, 60, 1–11, 2021.
- Karvonen, J., Simila, M., and Makynen, M.: Open water detection from Baltic Sea ice Radarsat-1 SAR imagery, IEEE Geoscience and Remote Sensing Letters, 2, 275–279, 2005.
 - Karvonen, J., Simila, M., and Lehtiranta, J.: SAR-based estimation of the Baltic sea ice motion, in: 2007 IEEE International Geoscience and Remote Sensing Symposium, pp. 2605–2608, IEEE, 2007.
 - Karvonen, J., Cheng, B., Vihma, T., Arkett, M., and Carrieres, T.: A method for sea ice thickness and concentration analysis based on SAR data and a thermodynamic model, The Cryosphere, 6, 1507–1526, 2012.
- 440 Karvonen, J. A.: Baltic sea ice SAR segmentation and classification using modified pulse-coupled neural networks, IEEE Transactions on Geoscience and Remote Sensing, 42, 1566–1574, 2004.
 - Kawamura, T., Shirasawa, K., Ishikawa, N., Lindfors, A., Rasmus, K., Granskog, M., Ehn, J., Leppäranta, M., Martha, T., and Vaikmäe, R.: Time-series observations of the structure and properties of brackish ice in the Gulf of Finland, Annals of Glaciology, 33, 1–4, 2001.
- Klais, R., Tamminen, T., Kremp, A., Spilling, K., An, B. W., Hajdu, S., and Olli, K.: Spring phytoplankton communities shaped by interannual weather variability and dispersal limitation: mechanisms of climate change effects on key coastal primary producers, Limnology and Oceanography, 58, 753–762, 2013.
 - Klais, R., Norros, V., Lehtinen, S., Tamminen, T., and Olli, K.: Community assembly and drivers of phytoplankton functional structure, Functional Ecology, 31, 760–767, 2017a.
- Klais, R., Otto, S. A., Teder, M., Simm, M., and Ojaveer, H.: Winter–spring climate effects on small-sized copepods in the coastal Baltic Sea, ICES Journal of Marine Science, 74, 1855–1864, 2017b.
 - Krikken, F., Schmeits, M., Vlot, W., Guemas, V., and Hazeleger, W.: Skill improvement of dynamical seasonal Arctic sea ice forecasts, Geophysical Research Letters, 43, 5124–5132, 2016.
 - Lemieux, J.-F., Beaudoin, C., Dupont, F., Roy, F., Smith, G. C., Shlyaeva, A., Buehner, M., Caya, A., Chen, J., Carrieres, T., et al.: The Regional Ice Prediction System (RIPS): verification of forecast sea ice concentration, Quarterly Journal of the Royal Meteorological Society, 142, 632–643, 2016.
 - Leppäranta, M.: On the structure and mechanics of pack ice in the Bothnian Bay, 1981.

- Leppäranta, M.: History and Future of Snow and Sea Ice in the Baltic Sea, in: Oxford Research Encyclopedia of Climate Science, 2023.
- Leppäranta, M. and Lewis, J.: Observations of ice surface temperature and thickness in the Baltic Sea, International Journal of Remote Sensing, 28, 3963–3977, 2007.
- 460 Leppäranta, M. and Myrberg, K.: Physical oceanography of the Baltic Sea, Springer Science & Business Media, 2009.
 - Löptien, U. and Axell, L.: Ice and AIS: ship speed data and sea ice forecasts in the Baltic Sea, The Cryosphere, 8, 2409–2418, 2014.
 - Luhamaa, A., Kimmel, K., Männik, A., and Rõõm, R.: High resolution re-analysis for the Baltic Sea region during 1965–2005 period, Climate dynamics, 36, 727–738, 2011.
- Mäkynen, M. and Hallikainen, M.: Passive microwave signature observations of the Baltic Sea ice, International Journal of Remote Sensing, 26, 2081–2106, 2005.
 - Mäkynen, M., Karvonen, J., Cheng, B., Hiltunen, M., and Eriksson, P. B.: Operational service for mapping the Baltic Sea landfast ice properties, Remote Sensing, 12, 4032, 2020.
 - Meehl, G. A., Goddard, L., Boer, G., Burgman, R., Branstator, G., Cassou, C., Corti, S., Danabasoglu, G., Doblas-Reyes, F., Hawkins, E., et al.: Decadal climate prediction: an update from the trenches, Bulletin of the American Meteorological Society, 95, 243–267, 2014.

- 470 Meier, H.: Regional ocean climate simulations with a 3D ice-ocean model for the Baltic Sea. Part 1: model experiments and results for temperature and salinity, Climate Dynamics, 19, 237–253, 2002.
 - Meier, H. M., Kniebusch, M., Dieterich, C., Gröger, M., Zorita, E., Elmgren, R., Myrberg, K., Ahola, M., Bartosova, A., Bonsdorff, E., et al.: Climate change in the Baltic Sea region: a summary, Earth System Dynamics Discussions, 2021, 1–205, 2021.
- Meier, H. M., Dieterich, C., Gröger, M., Dutheil, C., Börgel, F., Safonova, K., Christensen, O. B., and Kjellström, E.: Oceanographic regional climate projections for the Baltic Sea until 2100, Earth System Dynamics, 13, 159–199, 2022.
 - Meiners, K., Fehling, J., Granskog, M. A., and Spindler, M.: Abundance, biomass and composition of biota in Baltic sea ice and underlying water (March 2000), Polar biology, 25, 761–770, 2002.
 - Nielsen-Englyst, P., Høyer, J. L., Kolbe, W. M., Dybkjær, G., Lavergne, T., Tonboe, R. T., Skarpalezos, S., and Karagali, I.: A combined sea and sea-ice surface temperature climate dataset of the Arctic, 1982–2021, Remote Sensing of Environment, 284, 113 331, 2023.
- 480 Olason, E., Boutin, G., Korosov, A., Rampal, P., Williams, T., Kimmritz, M., Dansereau, V., and Samaké, A.: A new brittle rheology and numerical framework for large-scale sea-ice models, Journal of Advances in Modeling Earth Systems, 14, e2021MS002 685, 2022.
 - Omstedt, A. and Chen, D.: Influence of atmospheric circulation on the maximum ice extent in the Baltic Sea, Journal of Geophysical Research: Oceans, 106, 4493–4500, 2001.
 - Omstedt, A., Elken, J., Lehmann, A., and Piechura, J.: Knowledge of the Baltic Sea physics gained during the BALTEX and related programmes, Progress in Oceanography, 63, 1–28, 2004.

485

- Omstedt, A., Elken, J., Lehmann, A., Leppäranta, M., Meier, H., Myrberg, K., and Rutgersson, A.: Progress in physical oceanography of the Baltic Sea during the 2003–2014 period, Progress in Oceanography, 128, 139–171, 2014.
- Panteleit, T., Verjovkina, S., Jandt-Scheelke, S., Spruch, L., and Huess, V.: Baltic Sea Production Centre BALTIC-SEA MULTIYEAR PHY 003 011, innovation, 2, 22–8, 2019.
- 490 Parkinson, C. L.: Arctic sea ice, 1973-1976: Satellite passive-microwave observations, vol. 490, Scientific and Technical Information Branch, National Aeronautics and Space ..., 1987.
 - Pärn, O., Lessin, G., and Stips, A.: Effects of sea ice and wind speed on phytoplankton spring bloom in central and southern Baltic Sea, PLoS one, 16, e0242 637, 2021.
 - Pärn, O., Friedland, R., Rjazin, J., and Stips, A.: Regime shift in sea-ice characteristics and impact on the spring bloom in the Baltic Sea, Oceanologia, 64, 312–326, 2022.
 - Pemberton, P., Löptien, U., Hordoir, R., Höglund, A., Schimanke, S., Axell, L., and Haapala, J.: Sea-ice evaluation of NEMO-Nordic 1.0: a NEMO-LIM3. 6-based ocean-sea-ice model setup for the North Sea and Baltic Sea, Geoscientific Model Development, 10, 3105–3123, 2017.
 - Rasool, S. I., Menenti, M., and Bolle, H.-J.: Second assessment of climate change for the Baltic Sea basin, Springer, 2015.
- Raudsepp, U., Uiboupin, R., Maljutenko, I., Hendricks, S., Ricker, R., Liu, Y., Iovino, D., Peterson, K. A., Zuo, H., Lavergne, T., et al.: Combined analysis of Cryosat-2/SMOS sea ice thickness data with model reanalysis fields over the Baltic Sea, Journal of operational oceanography. Publisher: The Institute of Marine Engineering, Science & Technology, 12, S73—+, 2019.
 - Raudsepp, U., Uiboupin, R., Laanemäe, K., and Maljutenko, I.: Geographical and seasonal coverage of sea ice in the Baltic Sea, Copernicus Marine Service Ocean State Report, 2020.
- Figure 1982–2016, NAŠE MORE: znanstveni časopis za more i pomorstvo, 67, 53–59, 2020.

- Seina, A. and Peltola, J.: Duration of the Ice Season and Statistics of Fast Ice Thickness Along the Finnish Coast 1961-1990(Jaatalven Kestoaika-Ja Kiintojaan Paksuustilastoja Suomen Merialueilla 1961-1990), Finnish Marine Research FMRED 3, 258, 1991.
- Seinä, A., Grönvall, H., Kalliosaari, S., and Vainio, J.: Ice seasons 1996-2000 in Finnish sea areas. Jäätalvet 1996-2000 Suomen merialueilla, 2001.
 - Siitam, L., Sipelgas, L., Pärn, O., and Uiboupin, R.: Statistical characterization of the sea ice extent during different winter scenarios in the Gulf of Riga (Baltic Sea) using optical remote-sensing imagery, International journal of remote sensing, 38, 617–638, 2017.
 - Stigebrandt, A.: Physical oceanography of the Baltic Sea, in: A systems analysis of the Baltic Sea, pp. 19-74, Springer, 2001.
 - Team, B. A.: Assessment of climate change for the Baltic Sea basin, Springer Science & Business Media, 2008.
- Tuomi, L., Kanarik, H., Björkqvist, J.-V., Marjamaa, R., Vainio, J., Hordoir, R., Höglund, A., and Kahma, K. K.: Impact of ice data quality and treatment on wave hindcast statistics in seasonally ice-covered seas, Frontiers in Earth Science, 7, 166, 2019.
 - Vihma, T. and Haapala, J.: Geophysics of sea ice in the Baltic Sea: A review, Progress in oceanography, 80, 129–148, 2009.
 - Voipio, A.: The Baltic Sea, Elsevier, 1981.
- von Schuckmann, K., Le Traon, P.-Y., Smith, N., Pascual, A., Brasseur, P., Fennel, K., Djavidnia, S., Aaboe, S., Fanjul, E. A., Autret, E., et al.: Copernicus marine service ocean state report, Journal of Operational Oceanography, 11, S1–S142, 2018.
 - Wagner, P. M., Hughes, N., Bourbonnais, P., Stroeve, J., Rabenstein, L., Bhatt, U., Little, J., Wiggins, H., and Fleming, A.: Sea-ice information and forecast needs for industry maritime stakeholders, Polar Geography, 43, 160–187, 2020.
- Team (2008) Rasool et al. (2015) E.U. Copernicus Marine Service Information (CMEMS) (Accessed on 01 Dec 2023a) E.U. Copernicus Marine Service Information (CMEMS) (Accessed on 01 Dec 2023b) E.U. Copernicus Marine Service Information (CMEMS) (Accessed on 01 Dec 2023c) Granskog et al. (2006a) Granskog et al. (2003a) Granskog et al. (2003b) Granskog et al. (2006b) Haapala and Leppäranta (1996) HAAPALA and LEPPÄRANTA (1997) Haapala et al. (2015) Hersbach et al. (2020) Høyer and Karagali (2016) Høyer and She (2007) Jakacki and Meler (2019) Jevrejeva (2001) Jevrejeva et al. (2004) Jevrejeva and Leppäranta (2002) Jevrejeva and Moore (2001) Jevrejeva et al. (2003) Jylhä et al. (2008) Kärnä et al. (2021) Karvonen (2004) Karvonen (2013) Karvonen et al. (2012) Karvonen et al. (2005) Karvonen et al. (2007) Karvonen (2017) Karvonen (2021) Kawamura et al. (2001) Lemieux et al. (2016) Leppäranta (1981) Leppäranta and Lewis (2007) Leppäranta 530 and Myrberg (2009) Luhamaa et al. (2011) Mäkynen and Hallikainen (2005) Mäkynen et al. (2020) Meier (2002) Meier et al. (2022) Meier et al. (2021) Meiners et al. (2002) Nielsen-Englyst et al. (2023) Omstedt and Chen (2001) Omstedt et al. (2014) Omstedt et al. (2004) Panteleit et al. (2019) Pärn et al. (2022) Pemberton et al. (2017) Raudsepp et al. (2020) Rjazin and Parn (2020) Seinä et al. (2001) Seina and Peltola (1991) Stigebrandt (2001) Tuomi et al. (2019) Vihma and Haapala (2009) Voipio (1981) von Schuckmann et al. (2018) Parkinson (1987) Meehl et al. (2014) Hazeleger et al. (2013) Collins (2002) Fučkar et al. (2014) Krikken et al. (2016) Director et al. (2017) Raudsepp et al. (2019) Leppäranta (2023) Siitam et al. (2017) Löptien and Axell (2014) Klais et al. (2017a) Klais et al. (2017b) Pärn et al. (2021) Klais et al. (2013) Wagner et al. (2020) Åström et al.

(2024) Brodeau et al. (2024) Olason et al. (2022) Berglund and Molinier (2014)